Feature Article

Preparation of Fluorine-Doped Lead Dioxide Modified Electrodes for Electroanalytical Applications

Shiyun Ai, *Mengnan Gao*, *Wen Zhang*, *Zhengdong Sun*, *Litong Jin**

Department of Chemistry, East China Normal University, Shanghai 200062, P.R. China
* e-mail: chemashy@yahoo.com.cn

Received: May 30. 2002
Final version: September 24, 2002

Abstract
The effect of F^- on the modified films of lead dioxide in morphology and structure was studied. The results obtained by cyclic voltammetry (CV), X-diffractometer (XRD) and scanning electron microscope (SEM) techniques indicated that F^- could change the magnitude of lead dioxide crystal grain and the preferred crystallizing orientation on the substrate surface, even though it didn't change the basic structure of PbO_2. When the modified electrode was applied as an analytical sensor to determine phenolic compounds, the linearity was in the range of $2 \times 10^{-5} - 1 \times 10^{-3}$ mol/L and the detection limit was 2.5×10^{-6} mol/L. It was all found that the stability and reproducibility of the oxide-modified electrodes were improved by additional F^-.

Keywords: Lead dioxide, Fluoride, Anode, Phenol, Amperometry

1. Introduction

During the past decade, electrochemical methods [1–5] were developed to obtain the organic substance values by the oxidation of the organic compound on the surface of an electrode to, preferably, its elementary components (CO_2 and H_2O). The electrons released during the oxidation can be measured as electrical current, which is proportional to the organic values of the solution analyzed. Among these electrodes, there is a great interest in the development of lead dioxide as an anode electrode material with high electrocatalytic activity for anodic oxygen transfer processes [6–8]. Because lead dioxide is of high electrical conductivity, large oxygen overpotential, and chemical inertness in applications for electrolysis and electrosynthesis, it is favored as an anode material [9]. However, the application of lead dioxide is dependent upon its structure, morphology and phase composition, which are highly relied on the deposition method. Hence, many previous researches focused on the activity of the doped lead dioxide electrodes and found that this activity could be enhanced greatly by incorporation of some ions that modify lead dioxide. Several sets of data about the influence of foreign ions on the PbO_2 electrodeposition have been reported, such as Bi^{3+} [10–13], As^{3+} [14], Fe^{3+} [15–16], Cl^- [17], F^- [18], SO_4^{2-} [19]. Yet in most cases, details on the nature of the effect of these ions on the oxide electrodeposition are not known, although there is a vast literature on the mechanism of pure lead dioxide electrodeposition.

Among these dopants, F^- gave very good PbO_2 electrodes for oxygen transfer reactions. But the influence of F^- on the deposited of lead dioxide films in morphology and structure is almost neglected, and the incorporation of ionic species and their effects on the electrocatalytic activity of PbO_2 are still a matter of speculation.

Herein, the electrochemical modification of lead dioxide from solutions containing F^- was studied in this experiment. X-diffractometer (XRD) and scanning electron microscope (SEM) techniques were utilized to study the effect of F^- on the deposited films in morphology and structure of lead dioxide. The applications of this modified electrode as an analytical sensor to determine phenolic compounds were studied and satisfactory results were obtained.

2. Experimental

2.1. Reagents

All inorganic and organic reagents were obtained from commercial sources: Shanghai Chemical Reagent Co., China. All reagents were of analytical reagent grade quality. Stock solutions of Pb(II) and F^- were prepared in doubly distilled water from $Pb(NO_3)_2$ and NaF.

2.2. Apparatus

Cyclic voltammetry (CV) data and current-time (i-t) curves were performed on a CHI832 Electrochemical system (CHI, USA). All electrochemical experiment were carried out by a three-electrode cell with a saturated calomel electrode (SCE) as the reference electrode, a Pt wire electrode as the counter electrode and a Pt rotating disk electrode (Pt-RDE) as the working electrode.

  DOI: 10.1002/elan.200302667

X-ray data were collected using a D8ADVANCE X-ray power diffractometer (Bruker axs com. Ger.) based on Cu-Kα radiation. The 2θ (two-theta) angle of the diffractometer was stepped from 10° to 70° by 0.03° increments. Scanning electron micrograph (SEM) were obtained by a JSM-5610LV (JEOL) instrument.

2.3. Electrode Preparation

All experiments were performed at ambient temperature (25 ± 1 °C). The electrodes were mechanically polished with 0.05 μm alumina paste, rinsed with doubly distilled water, and then ultrasonicaly cleaned in water to remove the trapped alumina. The electrode area was 0.157 cm^2.

Prior to electrochemical modification, the bare Pt electrode was cycled within the range of 0.00 – 1.80 V at 100 mV s^{-1} in 1.0 mol/L $HClO_4$ solution until a reproducible background resulted. The PbO_2 and F-PbO_2 films were obtained via electrochemical modification in solutions of 1.0 mol/L $HClO_4$ and 10 mmol/L Pb(II) without or with the specified amounts of F^- by cycling the potential between 1.4 and 1.8 V at 100 mV s^{-1} for 30 cycles. After modification, the electrode was removed from the modifying solution and rinsed with doubly distilled water. All oxide films appeared to be shiny and black, uniform and with a thickness of 1 μm.

2.4. Data Analysis

Reactivity of electrode materials was evaluated according to the Koutecky-Levich equation:

$$1/I = 1/(nkFSc^b) + 1/(0.62\ nFSD^{2/3}\nu^{-1/6}c^b)\ 1/\omega^{1/2} \qquad (1)$$

where ν is the kinematic viscosity of the electrolyte solution ($cm^2\ s^{-1}$), ω is the angular velocity of electrode rotation (rad s^{-1}), S is the electrode area, n is the effective number of electrons exchanged in the reaction, k is the apparent heterogeneous rate constant. All other terms have their usual electrochemical significance.

Amperometric responses of the undoped PbO_2 electrode and F-PbO_2 modified electrode to phenol were measured as a steady state anodic current with a three-electrode system in a stirred 0.01 mol/L Na_2SO_4 solution by applying a potential of 1.4 V to the modified electrodes. The background current was allowed to decay to a steady value before phenol solution were added, and then the net increase of phenol oxidation current was measured as the response current.

3. Results and Discussion

3.1 Cyclic Voltammetry (CV) Experiments

Cyclic voltammogram (CV) obtained at the Pt-RDE electrode in the $HClO_4$ solution with the presence of only Pb(II) is shown in Figure 1A. At potential higher than 1.5 V, the anodic branch of the curve features an exponential current growth corresponding to the simultaneous reactions of Pb(II) oxidation and oxygen evolution. In the cathodic branch of the curve, a current peak due to the reduction of lead dioxide appears within the range of 1.0 – 1.2 V. According to Velicheuho [20], the area and the magnitude (I_p) of the reduction peak are good measures of the amount of lead dioxide deposited on the electrode surface.

Figure 1B shows the effect of the F^- ion concentration on the electrochemical modified lead dioxide film. As the concentration of F^- ion increased, the cathodic peak of the dissolution of lead dioxide reduced correspondingly. Thus it could be concluded that the formation of lead dioxide film becomes slower since the generation of PbF_3^- is enhanced, with the increase of F^- ion concentration. Which then slows down the crystallization of the electrodeposition film and

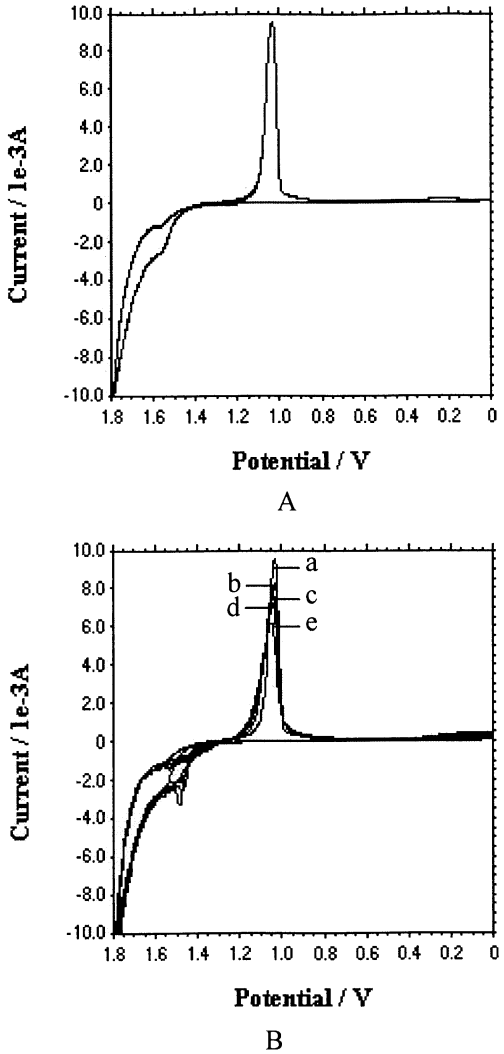

Fig. 1. Cyclic voltammograms (CV) in A) 1 mol/L $HClO_4$ + 0.01 mol/L Pb(II) and B) 1 mol/L $HClO_4$ + 0.01 mol/L Pb(II) with fluoride concentration of(a) 0.001, b) 0.002, c) 0.003, d) 0.004, e) 0.005 mol/L at the Pt-RDE electrode. Rotation velocity: 25 rad s^{-1}, potential scan rate: 100 mV s^{-1}.

Table 1. Rate constants for Pb(II) oxidation ($E = 1.800$ V)

Electrodeposition solution	$10^5 S$ [a] (m^2)	10^4 (m s^{-1})
1 mol/L $HClO_4$ + 0.01 mol/L Pb(II)	2.37	3.571
1 mol/L $HClO_4$ + 0.01 mol/L Pb(II) + 0.001 mol/L F^-	2.33	3.523
1 mol/L $HClO_4$ + 0.01 mol/L Pb(II) + 0.002 mol/L F	2.26	3.476
1 mol/L $HClO_4$ + 0.01 mol/L Pb(II) + 0.003 mol/L F^-	2.19	3.362

[a] S was determined from the slope of the $1/I$ versus $1/\omega^{1/2}$ straight lines (Eq. 1)

makes the grain of lead dioxide larger. According to Equation 1, a quantitative description of lead dioxide electrodeposition in the presence of additional ions is provided by the rate constant (k) of the deposition process, which is estimated from the intercepts the plot of $1/I$ versus $1/\omega^{1/2}$. Experimental and calculated kinetic data for the modification solution, in the absence and presence of foreign ions, are summarized in Table 1.

From Table 1, it is noted that with the increase of F^- ion concentration, the effective electrode area decreases, which makes the film in closer formation, thereby, firms the electrochemical modifying film. However, an excessive concentration of F^- ion would lead to only a very thin electrochemical modifying film or even no film. It is observed from Figure 1B, in the CV curve for solution containing 0.005 mol/L F^- ion, an anodic current peak appearing at 1.4 V, which could be the result of the oxidation of F^- in solution containing large concentration of F^- ion. Meanwhile, from Figure 1B, it is noted that with the increase of F^- ion concentration, the anodic current increased gradually in the exponential area, maybe due to the oxidation of Pb^{2+} and F^- and the oxygen evolution in this area.

3.2. Crystallographic Analysis of Films

Diffraction patterns of undoped PbO_2 films (A) and F-PbO_2 deposited films (B, C) on Pt substrates under a variety of conditions are shown in Figure 2. All the peaks obtained can be assigned to the rutile structure of β-PbO_2. But unlike the pattern for pure PbO_2, in the patterns for doped PbO_2, it was observed that relative peak intensity varies with the different concentrations of doping F^- ion, which was an indication of the variation in the preferred crystalline orientation on the substrate surface. For example, a higher peak intensity at $2\theta =$ ca. 25.727° appears in curve A, which gradient decreases with the increase of F^- ions concentration (curve B, C). Other peak intensities also have different changes in terms of the different concentrations of F^-.

As the F level increases in F-PbO_2, the diffraction peaks become narrower than that for undoped PbO_2, which indicated that the F-PbO_2 deposits have larger crystallite than undoped PbO_2, because diffraction peak width is inversely proportional to crystallite size [21]. Hence, it can be concluded that the presence of F^- in the modifying solution apparently decreases the rate of nucleation of the oxide crystallization on the Pt substrate, allowing individual crystallites to become larger. This conclusion is in correspondence with the above results of cyclic voltammetry and was confirmed by micrographs obtained by SEM of PbO_2 and F-PbO_2 which are shown in Figure 3. From Figure 3, it was also found that the crystallites of both undoped lead dioxide and fluorine-doped lead dioxide were well-distributed and all present in tetragonal rutile structure.

3.3. Oxidation of Phenols on F-PbO_2 Rotating Disk Electrode (RDE)

The catalytic effect of the doped lead dioxide electrode has generally been interpreted on the basis of the generation of surface activity sites with enhanced rates for anodic discharge of H_2O to produce adsorbed hydroxyl radicals ($^{\bullet}OH$) that are believed to be the requisite intermediate state of oxygen from H_2O in the anodic oxygen-transfer processes [22]. Linear regression statistics are given in Table 2 by Tafel plots according to Equation 2. In Equation 2, I_0 is the exchange current (μA), α_a is the anodic transfer coefficient, and η is the applied overpotential (V).

$$\log(I/\mu A) = \log(I_0/\mu A) + (\alpha_a n/0.059)\eta \quad (2)$$

The values of I_0 for the F-PbO_2 (6.18×10^{-6} A cm^{-2}) is larger than that for undoped PbO_2 (1.33×10^{-7} A cm^{-2}). This shows that the F-PbO_2 electrode catalyzes anodic oxygen-transfer reactions and will increase the rate of anodic discharge of H_2O.

Figure 4 shows the cyclic voltammetric curves obtained at undoped PbO_2 RDE and F-PbO_2 RDE in 0.01 mol/L Na_2SO_4 solution with or without 0.1 mmol/L phenol, respectively. For both electrodes, anodic production of O_2 occurred at a significant rate when $E > 1.8$ V. Following by addition of phenol, little increase in anodic current was observed for the undoped PbO_2 electrode (b), while a significant increase in anodic current was observed for the F-PbO_2 electrode (d) in comparison to the blank response (c). Furthermore, Koutecky-levich plots are shown in Figure 5 for background-corrected current values measured for phenol oxidation (1.4 V) at the Pt rotating disk electrodes covered with films of undoped PbO_2 and F-PbO_2 respectively. Meanwhile the theoretical plots for several values of n were calculated by assuming $D = 1.0 \times 10^{-5}$ cm^2 s^{-1} and $\nu = 0.010$ cm^2 s^{-1}. The intercepts of the experimental plots are very small, which is evidence for virtually transport-limited rates of oxidation at both undoped PbO_2 electrode and F-PbO_2 electrode.

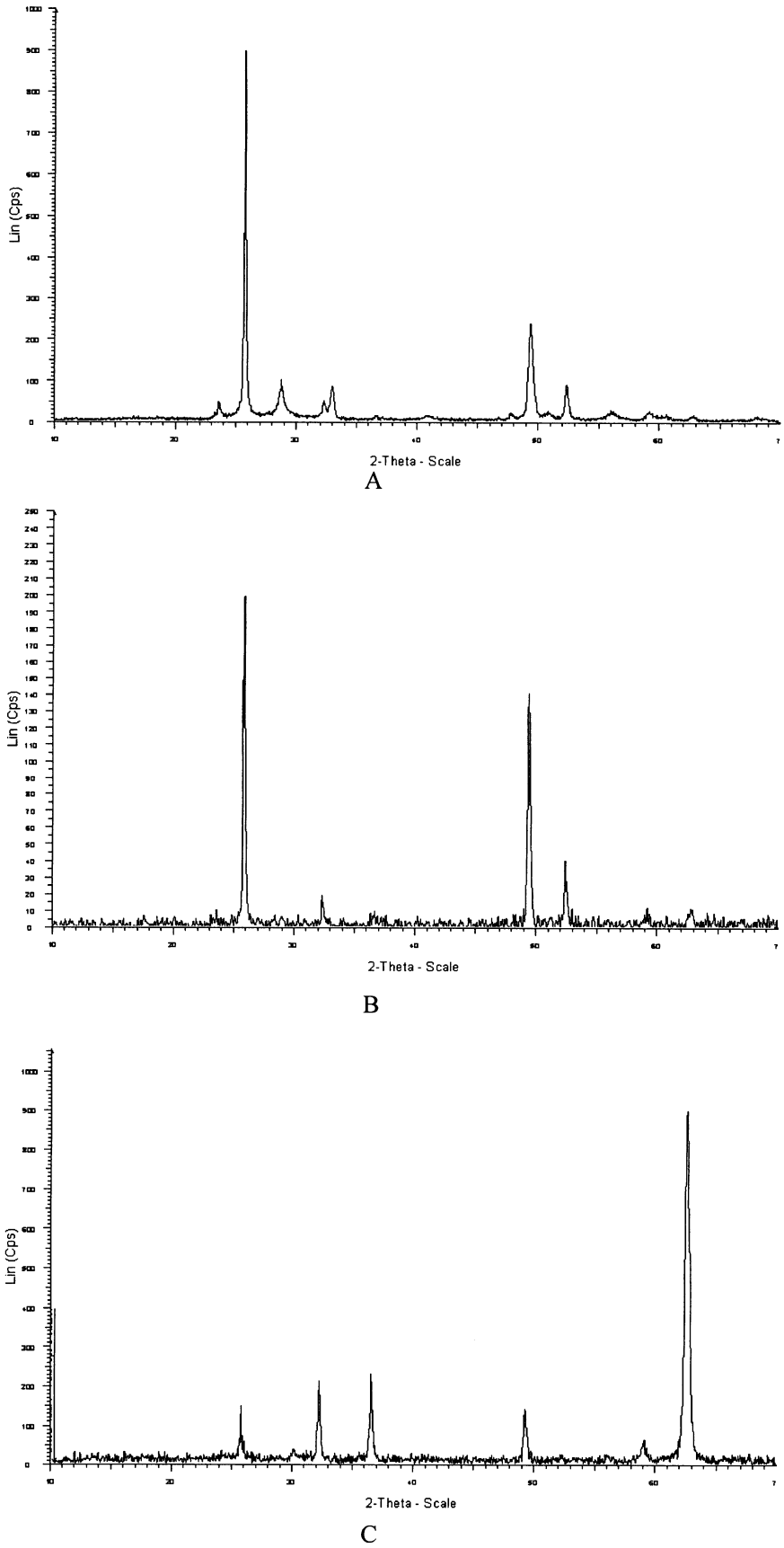

Fig. 2. X-ray diffraction patterns for undoped PbO_2 film (A) and F-PbO_2 deposited films (B: Pb^{2+}: 0.01 mol/L F^- 0.001 mol/L, C: Pb^{2+}: 0.01 mol/L F^- 0.002 mol/L) on Pt substrates under different of conditions.

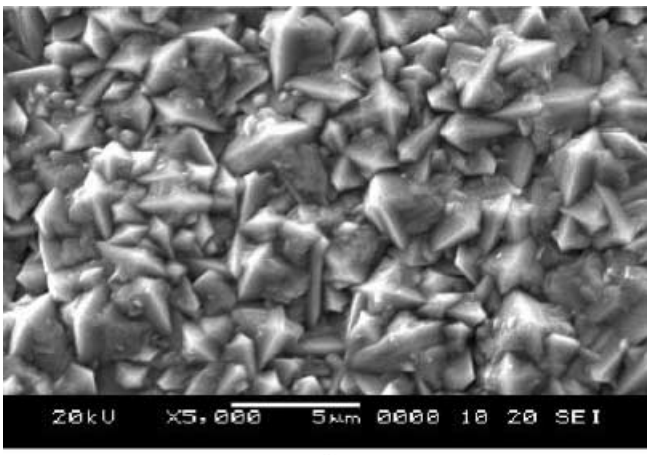

A

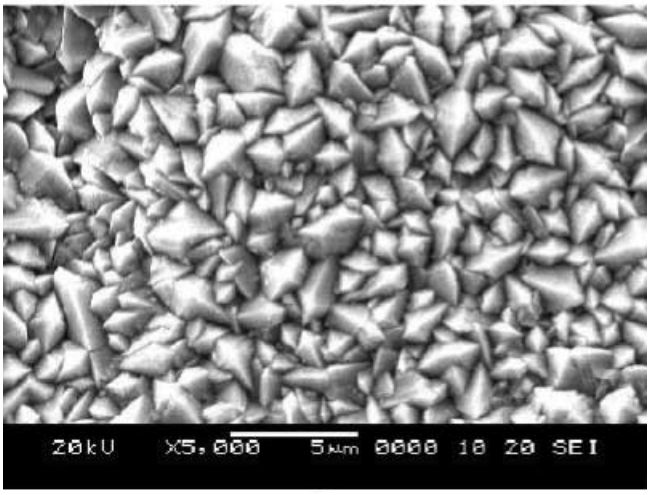

B

Fig. 3. SEM photographs for F-PbO_2 deposited film (A: Pb^{2+}: 0.01 mol/L F^- 0.002 mol/L) and undoped PbO_2 film (B).

Table 2. Linear regression statics for Tafel plots for O_2 evolution at various electrodes.

Electrode	I_0 [a] (A cm^{-2})	α_a *(eq* mol^{-1}*)*
PbO_2	1.33×10^{-7}	0.114
F-PbO_2 [b]	6.18×10^{-6}	0.086

[a] Tafel measurements: 1500 rev min^{-1} in deaerated 1.0 M $HClO_4$
[b] Pb^{2+}: 0.01 mol/L F^- 0.002 mol/L

However, the differences in the slopes of these plots indicate a significant difference in n values for phenol oxidation at the two electrodes. The values of k (cm s^{-1}) calculated from the intercepts of the plots are: $(1.3 \pm 0.5) \times 10^{-3}$ for PbO_2, $(11.6 \pm 1) \times 10^{-3}$ for F-PbO_2. This observation supports the presumption that the fluorine doped lead dioxide changes the activity sites in the host matrix (lead oxide) and increases the rate of anodic discharge of H_2O, which in turn enhances electrocatalytic activity of PbO_2 electrode.

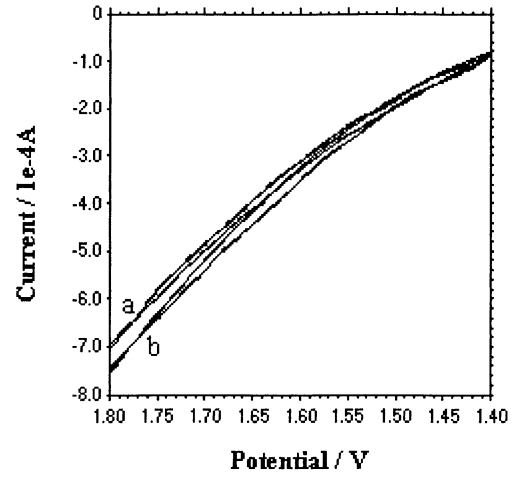

A

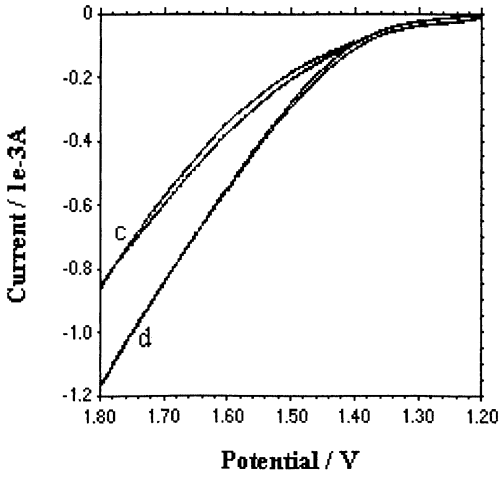

B

Fig. 4. Cyclic voltammogram (CV) of phenol at undoped PbO_2 electrode (A) and F-PbO_2 electrode (B). Rotation velocity: 25 rad s^{-1}, potential scan rate: 100 mV s^{-1}. a), c): 0 mmol/L phenol; b), d): 0.1 mmol/L phenol.

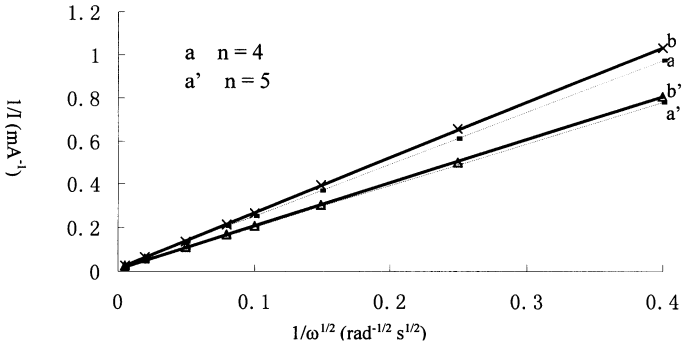

Fig. 5. Koutecky-Levich plot for the oxidation 0.1 mmol/L phenol in 1.0 mol/L $HClO_4$ on rotating disk electrode of the undoped PbO_2 (b) and F-PbO_2 (b′). Electrode potential: 1.8 V. Dashed lines represent calculated slopes for indicated values of n (a, a′); solid lines represent best fits to data.

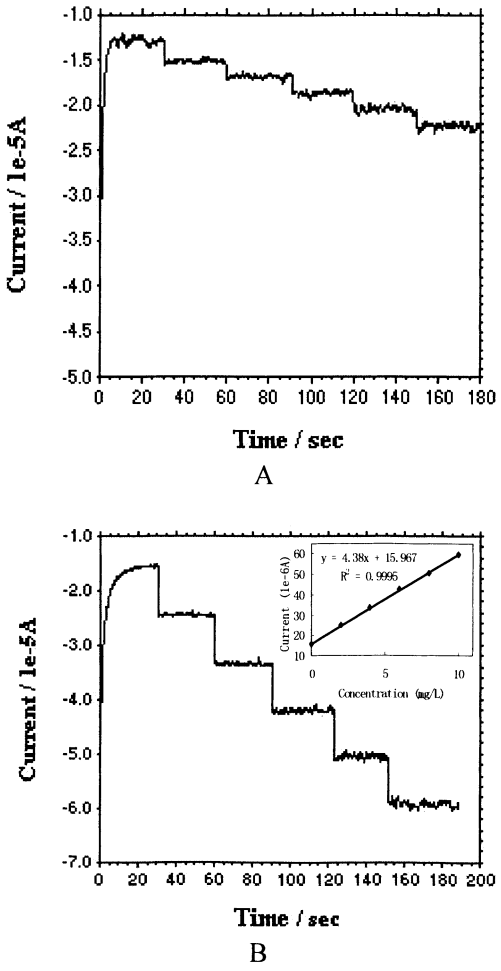

Fig. 6. Current-time recordings obtained on an increasing concentration in 2×10^{-5} mol/L step for phenol at undoped PbO_2 electrode (A) and F-PbO_2 electrode (B). Electrolyte: 0.01 mol/L Na_2SO_4; applied potential: +1.4 V (vs. SCE); rotation velocity: 25 rad s^{-1}.

3.4. Constant-Potential Amperometry in Stirred Solutions

Amperometry is a voltammetric technique for which the potential is kept constant over time [23]. It only requires simple measuring equipment, while the obtained current is a linear function of analytic concentration in solution. According to the mechanism of electrocatalytic O-transfer reactions, hydroxyl radicals (•OH) generated at the electrode surface by anodic discharge of H_2O can be adsorbed at specific surface sites, and then be transferred to oxidation products. Because the anodic discharge of H_2O at the F-PbO_2 electrode is greater than that at the undoped PbO_2 electrode, the response of phenol at the F-PbO_2 electrode is larger than that at the undoped PbO_2 electrode. This phenomenon also was proved in this experiment. Figure 6 shows the amperometric response of the undoped PbO_2 and F-PbO_2 electrode to the successive addition of 2×10^{-5} mol/L phenol in stirred 0.01 mol/L Na_2SO_4 solution at an operating potential of 1.4 V. The results show that the response of phenol on the F-PbO_2 electrode is larger than that on undoped PbO_2 electrode which is in agreement with the research premise presented above. The F-PbO_2 electrode shows fine linearity within the concentration range of $2 \times 10^{-5} - 1 \times 10^{-3}$ mol/L, with slope of 4.38 μA/mM, intercept of 16 μA, and correlation coefficient of 0.9995. The detection limit for phenol was 2.5×10^{-6} mol/L ($S/N = 3$).

The reproducibility of the phenol response of freshly prepared F-PbO_2 electrodes was determined by addition of 2×10^{-5} mol/L phenol in 0.01 mol/L Na_2SO_4 solution at 1.4 V. The response deteriorated slightly from addition to addition, and after 30 min the signal was equal to approximated 80% of the initial signal. However, after each determination, if the electrode was kept at a high potential 3.5 V for 3 min, the signal restored to its initial signal. This possibly suggests that fouling substances of phenol oxidative production at a high potential were demolished on the electrodes surface, and the electrodes surface was renewed. In addition, the undoped PbO_2 electrode does not remain stable to give a reproducible rest potential response for 1 day. The PbO_2 film slowly decomposes and the Pt surface is exposed, while on the other hand, the F-PbO_2 electrode remains stable and gave reproducible responses for about 60 days. Hence in this case F-PbO_2 electrode can be used effectively for quantitative estimation of phenol in millimolar concentration range.

4. Conclusions

According to the experimental results, it could be concluded that with the increase of the concentration of F^- ion in the modification solution, the rate of the formation of lead dioxide film decrease, thereby a suitable concentration of F^- ion in the modifying solution could make the grain of lead dioxide slightly become big and make the effective electrode areas decrease, which lead to form a firmer electrochemical modification film. The diffraction patterns demonstrate that F^- doesn't change the structure of PbO_2, but changes the preferred crystalline orientation of the modified crystallites on the substrate surface. According to voltammetric investigation, phenolic compounds could be easily oxidized at the operating potential (1.4 V versus saturated calomel electrode) at the F-PbO_2 modified electrodes. The amperometric measurement of phenol at 1.4 V at the F-PbO_2 electrode has a detection limit of 2.5×10^{-6} mol/L and shows fine linearity within the range of $2 \times 10^{-5} - 1 \times 10^{-3}$ mol/L. The F-PbO_2 electrode also shows long-term stability and reproducibility.

5. Acknowledgements

This work is supported by the National Natural Science Foundation of the People's Republic of China (No.20175006) and the Key Technology Research & Development Program of China (NO.2001BA210A04, NO.2002,AA601330).

6. References

[1] A. Ciszewski, G. Milczarek, *J. Electroanal. Chem.* **1999**, *469*, 18.
[2] F. Govaert, E. Temmerman, P. Kiekens, *Anal. Chim. Acta* **1999**, *385*, 307.
[3] I. G. Casella, M. Gatta, M. R. Guascito, T. R. I. Cataldi, *Anal. Chim. Acta* **1997**, *357*, 63.
[4] L. Nagy, G. Nagy, P. Hajós, *Sens. Actuators B* **2001**, *76*, 494.
[5] H. W. Lei, B. L. Wu, C. H. Cha, H. Kita, *J. Electroanal. Chem.* **1995**, *382*, 103.
[6] N. D. Popovic, D. C. Johuson, *Anal. Chem.* **1998**, *70*, 468.
[7] J. Ge, D. C. Johnson, *J. Electrochem. Soc.* **1995**, *142*, 1525.
[8] D. Velayutham, M. Noel, *Talanta* **1992**, *39*, 481.
[9] A. T. Kuhn, *Electrochemistry of Lead*, Academic Press, London **1979**.
[10] W. R. LaCourse, Y. L. Hsiao, D. C. Johnson, *J. Electrochem. Soc.* **1989**, *136*, 3714.
[11] K. L. Pamplin, D. C. Johnson, *J. Electrochem. Soc.* **1996**, *143*, 2119.
[12] K. Mondal, N. V. Mandich, S. B. Lalvani, *J. Appl. Electrochem.* **2001**, *31*, 165.
[13] N. D. Popovic, J. A. Cox, D. C. Johnson, *J. Electroanal. Chem.* **1998**, *455*, 153.
[14] I. H. Yeo, Y. S. Lee, D. C. Johnson, *Electrochim. Acta* **1992**, *37*, 1811
[15] A. B. Velichenko, R. Amadelli, G. L. Zucchini, D. V. Girenko, F. I. Danilov, *Electrochim. Acta* **2000**, *45*, 4341.
[16] C. A. S. Brevett, D. C. Johnson, *J. Electrochem. Soc.* **1992**, *139*, 1314.
[17] Y. L. Hsino, D. C. Johnson, *J. Electrochem. Soc.* **1989**, *136*, 3704.
[18] R. Amadelli, L. Armelao, A. B. Velichenko, N. V. Nikolenko, D. V. Girenko, S. V. Kovalyov, F. I. Danilov, *Electrochim. Acta* **1999**, *45*, 713.
[19] J. Feng, D. C. Johnson, *J. Electrochem. Soc.* **1990**, *137*, 507.
[20] A. B. Velichenko, D. V. Girenko, F. I. Danilov, *J. Electroanal. Chem.* **1996**, *405*, 127.
[21] I-H. Yeo, S. Kim, R. Jacobson, D. C. Johnson, *J. Electrochem. Soc.* **1989**, *136*, 1395.
[22] N. D. Popovic, J. A. Cox, D. C. Johnson, *J. Electroanal. Chem.* **1998**, *456*, 203.
[23] A. J. Bard, L. R. Faulkner, *Electrochemical Methods: Fundamentals and Applications*, Wiley, New York **1980**.

